AIMS Mathematics, 11(4): 12204–12232.
DOI: 10.3934/math.2026501
Received: 24 January 2026
Revised: 26 March 2026
Accepted: 10 April 2026
Published: 30 April 2026

http://www.aimspress.com/journal/Math

Research article

Analyzing finite-time convergence for variable-order fractional discrete dynamics in Degn–Harrison reaction–diffusion systems

Shaher Momani[1,2], Iqbal H. Jebril[3], Iqbal M. Batiha[2,3], Lina S. Calucag[4] and Anjan Biswas[6,7,8,9,*]

[1] Department of Mathematics, Faculty of Science, University of Jordan, Amman 11942, Jordan
[2] Nonlinear Dynamics Research Center (NDRC), Ajman University, Ajman 346, United Arab Emirates
[3] Department of Mathematics, Al-Zaytoonah University of Jordan, Amman 11733, Jordan
[4] Department of Mathematics and Science, University of Technology Bahrain, Salmabad 18041, Bahrain
[6] Department of Mathematics & Physics, Grambling State University, Grambling, LA 71245–2715, USA
[7] Department of Mathematics, Faculty of Science, Karadeniz Technical University, Trabzon–61080, Türkiye
[8] Department of Physics and Electronics, Khazar University, Baku, AZ–1096, Azerbaijan
[9] Department of Mathematics and Applied Mathematics, Sefako Makgatho Health Sciences University, Medunsa–0204, Pretoria, South Africa

* **Correspondence:** Email: biswas.anjan@gmail.com.

Abstract: This study presents a novel investigation into finite-time stability (FTS) and synchronization phenomena within a discrete reaction–diffusion system (RDS) governed by variable-order fractional (VOF) operators, inspired by the Degn–Harrison (D–H) model. By employing Caputo-type VOF differences, we model memory effects and time-varying dynamics typical of complex biological and chemical processes. Theoretical contributions include rigorous Lyapunov function (LF)-based criteria for establishing tempered Mittag-Leffler stability (MLS) and global FTS, as well as explicit expressions for the settling time T^*. A fractional-order (FO) error system is also analyzed, demonstrating that linear coupling ensures finite-time synchronization under variable-order conditions. Extensive numerical simulations confirm the theoretical predictions across various FO profiles $\delta(t)$ and parameter regimes. These findings bridge discrete fractional modeling with practical control strategies for systems exhibiting hereditary and anomalous diffusion effects.

Keywords: finite-time stability; variable-order fractional operators; reaction-diffusion systems;

Lyapunov methods; discrete Caputo difference; Mittag-Leffler stability

1. Introduction

The stability of reaction–diffusion systems (RDSes) has been extensively studied, leading to significant theoretical and numerical advancements. Spectral analysis reveals that singularly perturbed solutions possess a unique critical eigenvalue, which governs stability under small perturbations [1]. For spatially homogeneous oscillations, localized perturbations decay algebraically when no unstable linear modes exist [2]. Lyapunov function methods have been developed for binary RDSes. These methods link the time derivative of the functional to system eigenvalues [3] and establish optimal stability and instability conditions. One-dimensional systems with a single degree of freedom can exhibit multistability; however, solutions with multiple extrema are inherently unstable. Interestingly, such systems can possess more stable stationary states than homogeneous systems [4, 5]. Collectively, these approaches provide a robust framework for RDS stability analysis. Recent research has extended these concepts to discrete RDSes, with studies now focusing on stability analysis and numerical implementation. For example, [6] examined local and global stability in a discrete Gierer–Meinhardt model, and [7] analyzed finite -time stability (FTS) in generalized impulsive discrete systems for chemical and biological applications. In [8], the authors proved global exponential stability for noncritical wavefronts and algebraic stability for critical wavefronts in discrete systems with nonlocal delay effects. In [9], fully discrete RDS analogs were shown to preserve stability within invariant rectangular regions. These works utilized analytical tools such as Lyapunov function theory, finite difference schemes, and energy-based methods, supporting applications in biological pattern formation, chemical reactions, and microbial respiration.

Parallel work has focused on discrete fractional-order RDSes (FO-RDSes). These studies have examined the local and global asymptotic stability of equilibrium points through linearization and Lyapunov function methods [10, 11]. Applications include chemical models such as the Lengyel–Epstein system, epidemiological frameworks, neuronal modeling with FitzHugh–Nagumo systems, and glycolysis dynamics [12–14]. Discrete fractional calculus preserves essential continuous-time dynamics while also capturing discretization and FO effects [15–17]. Numerical simulations have been crucial for validating theoretical results and providing practical insights [18, 19]. Recently, FTS and synchronization in discrete FO-RDSs have gained increased attention. In [20], researchers derived FTS criteria for nonlinear systems with discrete time delays and demonstrated these properties in both Lengyel–Epstein and Degn–Harrison (D–H) systems. New lemmas were introduced in [21] to support finite-time synchronization controllers in D–H-type systems. Similarly, [22] studied FTS and synchronization in FO Lengyel–Epstein models using linearly interdependent controllers. These efforts leverage Lyapunov function theory and numerical evidence to demonstrate the efficacy of the proposed schemes, offering valuable insights for practical applications by providing ways to reach equilibrium points within prescribed time intervals in complex chemical and biological systems.

Beyond RDSes, recent years have witnessed significant progress in the analysis and numerical treatment of fractional differential equations across diverse nonlinear phenomena. For instance, the

dynamics of FO nonlinear dispersive wave systems have been effectively explored using homotopy-based techniques [23], and the time-fractional foam drainage equation has been thoroughly investigated through dynamical analysis and advanced numerical simulations [24]. These studies underscore the growing importance of combining analytical methods with robust numerical schemes to capture the complex behavior inherent in FO models. Motivated by such developments, the present work extends these methodological insights to the less-explored realm of VOF discrete RDSes, where both the fractional order and the spatial coupling evolve dynamically. However, despite these advances, the study of VOF discrete RDSes remains relatively unexplored. Most existing works assume constant fractional orders, which limits the modeling of systems with time-varying memory or hereditary effects. Recent developments in VOF calculus, such as those in [25], have enabled more accurate representations of complex dynamical processes, yet their application to discrete RDSes particularly in the context of FTS and synchronization, is still in its infancy.

This paper addresses these limitations by introducing a novel discrete VOF-RDS framework with several key theoretical advances beyond existing works:

- **Novel VOF formulation**: Unlike constant-order fractional models, our approach incorporates time-varying fractional orders $\delta(t)$, enabling dynamic adaptation to changing system memory characteristics and providing more realistic modeling of biological and chemical processes with evolving diffusion properties.
- **Advanced stability theory**: We establish tempered Mittag-Leffler stability (MLS) criteria for VOF systems, extending beyond classical Mittag-Leffler stability results. Our approach provides explicit settling time expressions T^* that remain valid under order variations, addressing a key limitation of constant-order frameworks.
- **Robust synchronization analysis**: Whereas prior work demonstrated synchronization for constant-order systems, we prove finite-time synchronization under variable-order conditions by developing new fractional Lyapunov estimates that accommodate time-varying memory effects, thereby providing more flexible control strategies.
- **Comprehensive numerical framework**: We develop a complete discretization scheme for VOF-RDSes, including novel interpolation techniques for nongrid temporal evaluations and specialized numerical operators for variable-order Caputo differences, enabling practical implementation of our theoretical results.

The main contributions of this work are as follows:

- A novel discrete VOF-RDS formulation using Caputo-type differences with time-varying order $\delta(t)$, providing superior modeling of memory-dependent processes compared to constant-order approaches.
- Rigorous Lyapunov-based criteria for tempered MLS and global finite-time stability in VOF systems, with explicit settling time T^* expressions that generalize constant-order results.
- Analytical proof of finite-time synchronization via linear internode coupling in VOF settings, extending synchronization controllers to handle time-varying fractional orders.
- A comprehensive numerical framework demonstrating the practical implementation and validation of our theoretical results under realistic variable-order conditions.

The main novelty of the proposed VOF discrete D–H model lies in several key advancements over previously published integer-order [26–28] and constant-order fractional models [29]. First, unlike

constant-order frameworks, the time-varying VOF captures nonstationary memory effects and evolving diffusion characteristics (e.g., transitions between superdiffusion and subdiffusion) inherent in real biological and chemical processes. Second, whereas prior discrete fractional reaction–diffusion studies focused on asymptotic stability [9, 10] or finite-time results for constant orders [18, 19, 22], we establish rigorous Lyapunov-based criteria for both tempered Mittag-Leffler stability and global finite-time stability under variable-order dynamics, including explicit settling time expressions T^* that remain valid under order variations. Third, we prove finite-time synchronization via linear coupling, an aspect not addressed in previous variable-order reaction–diffusion works. Finally, the discrete formulation with Caputo-type variable-order differences, together with a complete numerical discretization scheme, bridges the gap between advanced fractional calculus and practical implementation, providing a more flexible and realistic tool for modeling complex, time-varying hereditary processes. This paper studies FTS and synchronization in a discrete VOF-RDS based on the D–H model. We combine VOF calculus with Lyapunov function (LF) analysis to establish rigorous stability criteria, which we verify through numerical simulations. The paper is organized as follows: Section 2 introduces the model formulation, including VOF operators and the discretized system dynamics. Section 3 details the key theoretical contributions on MLS and FTS, supported by Lyapunov-based proofs. Section 4 illustrates the validity of the theoretical framework through simulations and demonstrates the system's FTS behavior.

2. Model formulation

To illustrate the necessity of VOF operators, consider drug diffusion through heterogeneous biological tissues. In such systems, the diffusion characteristics change over time due to factors such as tissue hydration, pH variations, and cellular uptake. A constant-order fractional model with fixed δ cannot capture these temporal changes in memory effects. For example, as drug concentration saturates tissue regions, the diffusion may transition from superdiffusive ($\delta > 1$) to subdiffusive ($\delta < 1$) behavior. Our VOF framework with $\delta(t)$ naturally accommodates such transitions, whereas constant-order models would either overestimate or underestimate drug penetration rates at different temporal stages. Another critical example arises in neural dynamics with synaptic plasticity. During learning processes, the memory retention properties of neural networks evolve, requiring time-varying fractional orders to accurately model the changing persistence of neural activities. Constant-order models fail to capture this adaptive memory behavior, leading to inaccurate predictions of synchronization and stability in neural populations.

The D–H model has been widely studied for its stability and pattern formation properties. Researchers have focused on finding conditions for asymptotic stability, with recent studies establishing weaker conditions than previously known [26]. The asymptotic stability of unique constant equilibrium points has been demonstrated using contracting rectangles and Lyapunov functions [27]. Pattern formation has been analyzed through Turing instability and Hopf bifurcation theory, revealing nonhomogeneous stationary and periodic solutions [28]. A time-FO version of the model has also been developed, which provides better dynamic representations and deeper system insights. Sufficient conditions for asymptotic stability of the FO model have been established using multiple methods, including invariant rectangles, stability theory, linearization, and Lyapunov-based approaches [29]. Together, these studies improve our understanding of the D–H model's dynamics

and stability. The governing dynamics of the classical model are given by:

$$\begin{cases} \dfrac{\partial u(x,t)}{\partial t} = k_1 \Delta u + b_1 - u - \dfrac{vu}{1+qu^2}, \\ \dfrac{\partial v(x,t)}{\partial t} = k_2 \Delta v + b_2 - \dfrac{vu}{1+qu^2}, \qquad (x,t) \in \Omega \times \mathbb{R}^+. \\ \dfrac{\partial u}{\partial \mathbf{n}}\Big|_{\partial\Omega} = \dfrac{\partial v}{\partial \mathbf{n}}\Big|_{\partial\Omega} = 0, \\ u(x,0) = u_0(x), \quad v(x,0) = v_0(x), \end{cases} \tag{2.1}$$

Here, $\Omega \subset \mathbb{R}^n$ is a bounded domain with smooth boundary $\partial\Omega$. The vector $\mathbf{n}$ is the outward unit normal. The parameters $k_1, k_2 > 0$ are diffusion coefficients; $q > 0$ controls sigmoidal nonlinearity; and b_1, b_2 are basal production rates. The Laplacian operator $\Delta = \sum_{i=1}^{n} \partial^2/\partial x_i^2$ models spatial diffusion, where $x = (x_1, x_2, \ldots, x_n)$ are the spatial coordinates. Neumann boundary conditions ensure mass conservation.

To include memory effects and model non-Fickian transport in biological media, we reformulate the system using VOF derivatives [30]. Recent research has employed Caputo-type derivatives with variable FO to model complex nonlinear systems. For example, [31] demonstrated the effectiveness of this approach in a Lotka–Volterra predator–prey model, establishing the existence and uniqueness of solutions. In [32], three types of Caputo–Hadamard variable-order derivatives were introduced, and the authors provided approximation formulas along with error estimates. Further, [33] extended the continuation theorem for VOF differential equations, proving global existence and Ulam–Hyers stability results. In [34], numerical approximations for three Caputo VOF types were developed, accompanied by error analyses and applications to fractional-order partial differential equations (FO-PDEs). The choice of the Caputo-type VOF difference operator is motivated by several theoretical and practical considerations. First, Caputo-type differences allow the incorporation of standard integer-order initial conditions (e.g., $u(a)$, $v(a)$), which are physically meaningful and directly measurable in experiments, a property not shared by the Riemann–Liouville operator. Second, the Caputo operator satisfies ${}^{\mathrm{C}}\Delta_a^{\delta(t)}(\text{constant}) = 0$, a crucial feature for Lyapunov stability analyses because it ensures that equilibrium points remain stationary under the fractional dynamics. Third, the kernel of the Caputo difference is weakly singular yet integrable, providing a natural framework for modeling subdiffusive and superdiffusive processes while maintaining compatibility with the discrete fractional calculus literature [35]. Alternative operators, such as the Grünwald–Letnikov difference, are computationally more demanding for variable-order implementations and do not simplify Lyapunov estimates as elegantly; the Atangana–Baleanu operator, although capable of representing nonsingular kernels, introduces a Mittag-Leffler function in the kernel that increases numerical complexity and is less established for Lyapunov-based FTS in discrete settings. Thus, the Caputo formulation strikes an optimal balance between mathematical tractability, physical interpretability, and computational feasibility for the stability and synchronization analyses pursued in this work.

The classical D–H model (2.1) assumes Fickian diffusion and instantaneous dynamics, which may be insufficient for systems where diffusion is anomalous or where memory effects influence reaction kinetics. To overcome these limitations, we replace the integer-order time derivatives with

Caputo-type VOF differences, yielding a discrete VOF-RDS formulation. The VOF is allowed to vary with time, providing a flexible tool to model evolving diffusion regimes: For instance, in drug transport through heterogeneous biological tissues, the diffusion exponent may shift from superdiffusive ($\delta(t) > 1$) during initial penetration to subdiffusive ($\delta(t) < 1$) as the drug binds to cellular components. Similarly, in neural dynamics with synaptic plasticity, the memory retention of the network changes during learning, requiring a time-varying FO to capture the adaptation. The use of variable-order operators thus embeds non-Fickian transport and history-dependent reactions directly into the discrete reaction–diffusion framework, making the model more faithful to the underlying biophysical processes than constant-order fractional or integer-order alternatives.

Definition 1 ([35]). *The Taylor monomial of VOF is given by*

$$h_{\delta(t)}(t, s) = \frac{(t-s)^{(\delta(t))}}{\Gamma(1+\delta(t))}, \tag{2.2}$$

where

$$t^{(\delta(t))} = \frac{\Gamma(t+1)}{\Gamma(t+1-\delta(t))}.$$

Definition 2 ([35]). *Let $u : \mathbb{N}_a \to \mathbb{R}$ be a given function and $\delta(t) > 0$. Then, the VOF sum is defined as follows:*

$$\Delta_a^{-\delta(t)} u(t) = \sum_{s=a}^{t-\delta(t)} h_{\delta(t)-1}(t, s+1) u(s), \quad \forall t \in \mathbb{N}_{a+\delta(t)}. \tag{2.3}$$

Definition 3 ([36]). *The VOF in terms of Caputo calculus is given by:*

$${}^{C}\Delta_a^{\delta(t)} u(t) = \frac{1}{\Gamma(m-\delta(t))} \sum_{s=a}^{t-(m-\delta(t))} (t-s-1)^{(m-\delta(t)-1)} \Delta^m u(s), \tag{2.4}$$

where $u : \mathbb{N}_a := \{a, a+1, a+2, \ldots\} \to \mathbb{R}, \delta(t) \neq \mathbb{N}, m = [\delta(t)] + 1$, and $t \in \mathbb{N}_{a+m-\delta(t)}$.

The Caputo-type VOF forward difference ${}^{C}\Delta_a^{\delta(t)}$ supplants classical derivatives:

$$\begin{cases} {}^{C}\Delta_a^{\delta(t)} u(x,t) = k_1 \Delta u + b_1 - u - \dfrac{vu}{1+qu^2}, \\ {}^{C}\Delta_a^{\delta(t)} v(x,t) = k_2 \Delta v + b_2 - \dfrac{vu}{1+qu^2}. \end{cases} \tag{2.5}$$

For computational discretization, we partition $\Omega = [0, L]$ uniformly with step size Δ_x. With m nodes ($x_{i+1} = x_i + \Delta_x$, $i = 0, \ldots, m$), the forward difference is defined in [6] as:

$$\tilde{\Delta}\vartheta_i(t) = \vartheta_{i+1}(t) - \vartheta_i(t). \tag{2.6}$$

Then,

$$\Delta\vartheta(x,t) \approx \frac{\vartheta_{i-1}(t) - 2\vartheta_i(t) + \vartheta_{i+1}(t)}{\Delta_x^2} \equiv \frac{\tilde{\Delta}^2\vartheta_{i-1}(t)}{\Delta_x^2}. \tag{2.7}$$

Applying this spatial discretization to (2.5) yields semidiscrete dynamics at node i:

$$\begin{cases} {}^{C}\Delta_a^{\delta(t)} u_i(t) = \dfrac{k_1}{\Delta_x^2}\tilde{\Delta}^2 u_{i-1}(\varsigma_t) + b_1 - u_i(\varsigma_t) - \dfrac{v_i(\varsigma_t)u_i(\varsigma_t)}{1+qu_i^2(\varsigma_t)}, \\ {}^{C}\Delta_a^{\delta(t)} v_i(t) = \dfrac{k_2}{\Delta_x^2}\tilde{\Delta}^2 v_{i-1}(\varsigma_t) + b_2 - \dfrac{v_i(\varsigma_t)u_i(\varsigma_t)}{1+qu_i^2(\varsigma_t)}, \end{cases} \tag{2.8}$$

where $\varsigma_t = t + \delta(t) - 1$. Periodic constraints enforce spatial coherence:

$$\begin{cases} u_{j-1}(t) = u_{m+j-1}(t), \\ v_{j-1}(t) = v_{m+j-1}(t), \quad j = 1, 2. \end{cases} \tag{2.9}$$

Initial profiles are sampled as:

$$u_i(a) = u_0(x_i), \quad v_i(a) = v_0(x_i). \tag{2.10}$$

The system exhibits a uniform equilibrium point (EP) solution (u^*, v^*) solving:

$$\begin{cases} b_1 - u^* - \dfrac{v^*u^*}{1+q(u^*)^2} = 0, \\ b_2 - \dfrac{v^*u^*}{1+q(u^*)^2} = 0, \end{cases} \tag{2.11}$$

reducible to the unique EPs

$$(u^*, v^*) = \left(b_1 - b_2,\ b_2\frac{1+q(b_1-b_2)^2}{b_1-b_2}\right), \quad b_1 \neq b_2. \tag{2.12}$$

Linear stability assessment requires solving the spectral problem for the discrete Laplacian:

$$\begin{cases} \tilde{\Delta}^2\psi_{i-1}(\varsigma_t) = -\mu_i\psi_i(\varsigma_t), \\ \psi_0(t) = \psi_m(t), \\ \psi_1(t) = \psi_{m+1}(t), \end{cases} \tag{2.13}$$

where μ_i are wavenumber-dependent eigenvalues. Substituting μ_i into (2.13) decouples modal dynamics:

$$\begin{cases} {}^{C}\Delta_a^{\delta(t)} u_i(t) = -\dfrac{k_1\mu_i}{\Delta_x^2}u_i(\varsigma_t) + b_1 - u_i(\varsigma_t) - \dfrac{v_i(\varsigma_t)u_i(\varsigma_t)}{1+qu_i^2(\varsigma_t)}, \\ {}^{C}\Delta_a^{\delta(t)} v_i(t) = -\dfrac{k_2\mu_i}{\Delta_x^2}v_i(\varsigma_t) + b_2 - \dfrac{v_i(\varsigma_t)u_i(\varsigma_t)}{1+qu_i^2(\varsigma_t)}. \end{cases} \tag{2.14}$$

Remark 1. *Unlike classical integer-order models, which are Markovian and lack long-term memory, the VOF formulation embeds time-dependent memory effects through the kernel of the Caputo difference. In constant-order fractional models, the memory depth is fixed by a constant δ, limiting the ability to describe processes where the underlying transport or reaction kinetics evolve over time. The present framework with time-varying $\delta(t)$ overcomes this limitation by continuously adjusting the weight assigned to past states, allowing the system to transition between subdiffusive ($\delta(t) < 1$) and*

superdiffusive ($\delta(t) > 1$) regimes as needed. From a stability perspective, the variable-order dynamics preserve the finite-time convergence properties established in Theorems 1 and 4, provided $\delta(t)$ remains within an interval $(\delta_1, \delta_2) \subset (0, 1)$. The settling time T^* is influenced by the infimum of $\delta(t)$: a lower average order tends to accelerate the theoretical convergence bound, as verified numerically in Cases 1–4. Constant-order models, by contrast, fix δ and thus lose the ability to adapt the memory characteristic during system evolution. Moreover, integer-order models ($\delta = 1$) generally yield exponential convergence without the finite-time extinction property observed here. Hence, the variable-order formulation offers greater flexibility and realism for systems with evolving hereditary or anomalous diffusion properties, while still admitting rigorous Lyapunov-based stability criteria.

3. Main results

In this section, we establish the main theoretical results concerning the dynamics and stability of the VOF-RDS. We begin by analyzing the properties of the nonlinear reaction terms and derive sufficient conditions ensuring tempered MLS and FTS. The theoretical findings are supported by Lyapunov-based methods and fractional discrete calculus tools.

Lemma 1 ([21])**.** *The reaction term satisfies the uniform Lipschitz condition:*

$$\left| \frac{v_i(t)u_i(t)}{1 + qu_i^2(t)} - \frac{v^*u^*}{1 + qu^{*2}} \right| \leq Q \left(|u_i(t) - u^*| + |v_i(t) - v^*| \right), \tag{3.1}$$

where

$$Q \geq \max \left\{ \frac{5}{4}k, \ \frac{1}{2\sqrt{q}} \right\}, \quad |v^*| < k.$$

Theorem 1. *Consider the system:*

$${}^{C}\Delta_a^{\delta(t)}\vartheta(t) = V(\varsigma_t, \vartheta(\varsigma_t)), \tag{3.2}$$

where we define $\varsigma_t := t + \delta(t) - 1$. If there exist a LF $V : \mathbb{N}_{a+1-\delta_2} \times D \to \mathbb{R}^+$ and parameters $0 < \delta_1 < \delta(t) < \delta_2 < 1$, $b, c, q_1, q_2, q_3 > 0$ satisfying

$$q_1\|\vartheta(t)\|^b \leq V(t, \vartheta(t)) \leq q_2\|\vartheta(t)\|^{bc}, \tag{3.3}$$

$${}^{C}\Delta_a^{\delta(t)}V(t, \vartheta(t)) \leq -q_3\|\vartheta(\varsigma_t)\|^{bc}, \tag{3.4}$$

$\forall t \in \mathbb{N}_{a+1}$ and $\vartheta(t) \in D \setminus \{0\}$, then the EP of system (3.2) *is tempered MLS.*

Proof. We apply the Lyapunov direct method to establish tempered MLS. From (3.3):

$$\|\vartheta(\varsigma_t)\|^{bc} \geq \frac{V(\varsigma_t, \vartheta(\varsigma_t))}{q_2}. \tag{3.5}$$

Substituting into (3.4) yields:

$${}^{C}\Delta_a^{\delta(t)}V(t, \vartheta(t)) \leq -\frac{q_3}{q_2}V(\varsigma_t, \vartheta(\varsigma_t)). \tag{3.6}$$

Define $\lambda := q_3/q_2 > 0$, giving:

$$ {}^{C}\Delta_a^{\delta(t)} V(t) \leq -\lambda V(\varsigma_t). \tag{3.7}$$

Consider the comparison equation:

$$ {}^{C}\Delta_a^{\delta(t)} u(t) = -\lambda u(\varsigma_t), \quad u(a) = V(a, \vartheta(a)). \tag{3.8}$$

Its solution is:

$$ u(t) = u(a) E_{\delta(t)}(-\lambda, t-a), \tag{3.9}$$

where the discrete Mittag-Leffler function is defined as:

$$ E_{\delta(t)}(\lambda, t-a) = \sum_{k=0}^{\infty} \lambda^k \frac{(t-a)^{(k\delta(t))}}{\Gamma(1+k\delta(t))}, $$

By the comparison principle for variable-order fractional difference equations (see [35] for the constant-order case, extended to variable-order through continuity and kernel properties), we have:

$$ V(t, \vartheta(t)) \leq V(a, \vartheta(a)) E_{\delta(t)}(-\lambda, t-a). \tag{3.10}$$

The extension to variable-order operators is justified by the continuity of the solution with respect to the fractional order parameter and the positivity of the kernel functions in the Caputo-type difference operator. For variable-order systems, the comparison principle holds under the condition that the fractional order $\delta(t)$ varies smoothly and remains within the interval $(\delta_1, \delta_2) \subset (0, 1)$.

Combining (3.3) and (3.10):

$$ q_1 \|\vartheta(t)\|^b \leq V(t, \vartheta(t)) \leq q_2 \|\vartheta(a)\|^{bc} E_{\delta(t)}(-\lambda, t-a). \tag{3.11}$$

Thus,

$$ \|\vartheta(t)\|^b \leq \frac{q_2}{q_1} \|\vartheta(a)\|^{bc} E_{\delta(t)}(-\lambda, t-a). \tag{3.12}$$

Because $b > 0$ and both sides of the inequality are non-negative (as norms and the Mittag-Leffler function with negative argument are non-negative), the function $x \mapsto x^{1/b}$ is well-defined and strictly increasing on $[0, \infty)$. Therefore, applying this monotonic function to both sides preserves the inequality direction:

$$ \|\vartheta(t)\| \leq \left(\frac{q_2}{q_1}\right)^{1/b} \|\vartheta(a)\|^c \left[E_{\delta(t)}(-\lambda, t-a)\right]^{1/b}. \tag{3.13}$$

This yields the form:

$$ \|\vartheta(t)\| \leq \mu \left[E_{\delta(t)}(-\lambda, t-a)\right]^{\gamma} \|\vartheta(a)\|^{\beta}, \tag{3.14}$$

where $\mu = (q_2/q_1)^{1/b}$, $\gamma = 1/b$, $\beta = c$. Because μ is constant, for any $\epsilon > 0$ and $\tau \geq 0$,

$$ \mu \leq \mu e^{\epsilon\tau}, \tag{3.15}$$

confirming that μ is tempered. Thus, the zero solution is tempered MLS. □

Remark 2. *Although the VOF $\delta(t)$ is time-varying in the interval (δ_1, δ_2), the Lyapunov condition utilizes the upper bound δ_2. This ensures that the decay estimate remains valid due to δ_2 dominating the effective decay rate.*

Lemma 2. *For any $e : \mathbb{N}_{a+1} \to \mathbb{R}$, $\delta(t) \in (0, 1)$, $a \in \mathbb{R}$, and $t \in \mathbb{N}_a$, it holds that*

$$ {}^{C}\Delta_a^{\delta(t)}|e(t)| \leq \operatorname{sgn}(e(t))\, {}^{C}\Delta_a^{\delta(t)} e(t). \tag{3.16}$$

Proof. The Caputo FO difference is defined as:

$$ {}^{C}\Delta_a^{\delta(t)} e(t) = \frac{1}{\Gamma(1-\delta(t))} \sum_{s=a}^{t-1} (t-s-1)^{(-\delta(t))} \Delta e(s), $$

where

$$ (t-s-1)^{(-\delta(t))} = \frac{\Gamma(t-s)}{\Gamma(t-s+\delta(t))}. $$

Because $\Gamma(1-\delta(t)) > 0$, it suffices to prove the inequality

$$ \sum_{s=a}^{t-1} k(s)\Delta|e(s)| \leq \operatorname{sgn}(e(t)) \sum_{s=a}^{t-1} k(s)\Delta e(s), \tag{3.17}$$

where the kernel is defined by

$$ k(s) = (t-s-1)^{(-\delta(t))}. \tag{3.18}$$

Define the auxiliary function

$$ \mathscr{H}(s) = |e(s)| \cdot \mathbf{1}_{\{\operatorname{sgn}(e(s)) \neq \operatorname{sgn}(e(t))\}}. \tag{3.19}$$

Then, the absolute value of $e(s)$ can be expressed as:

$$ |e(s)| = \operatorname{sgn}(e(t)) \cdot e(s) + 2\mathscr{H}(s), \tag{3.20}$$

and hence, its forward difference satisfies:

$$ \Delta|e(s)| = \operatorname{sgn}(e(t)) \cdot \Delta e(s) + 2\Delta\mathscr{H}(s). \tag{3.21}$$

Substituting into the weighted sum yields:

$$ \sum_{s=a}^{t-1} k(s)\Delta|e(s)| = \operatorname{sgn}(e(t)) \sum_{s=a}^{t-1} k(s)\Delta e(s) + 2\sum_{s=a}^{t-1} k(s)\Delta\mathscr{H}(s). \tag{3.22}$$

Thus, to establish the desired inequality, it remains to show that

$$ \sum_{s=a}^{t-1} k(s)\Delta\mathscr{H}(s) \leq 0. \tag{3.23}$$

Note that $\mathscr{H}(t) = 0$. Using the summation-by-parts identity, we write

$$\begin{aligned}\sum_{s=a}^{t-1} k(s)\Delta\mathscr{H}(s) &= \sum_{s=a+1}^{t} k(s-1)\mathscr{H}(s) - \sum_{s=a}^{t-1} k(s)\mathscr{H}(s) \\ &= -k(a)\mathscr{H}(a) + \sum_{s=a+1}^{t-1} \mathscr{H}(s)\left(k(s-1) - k(s)\right).\end{aligned} \tag{3.24}$$

The kernel $k(s)$ is increasing in s because the function $x \mapsto \Gamma(x)/\Gamma(x+\delta)$ is decreasing for $\delta > 0$. This follows from the ratio:

$$\frac{k(s)}{k(s-1)} = 1 + \frac{\delta(t)}{t-s} > 1, \tag{3.25}$$

which implies

$$k(s-1) - k(s) \leq 0. \tag{3.26}$$

Because $\mathscr{H}(s) \geq 0$, $\mathscr{H}(a) \geq 0$, and $k(a) > 0$, it follows that:

$$-k(a)\mathscr{H}(a) \leq 0. \tag{3.27}$$

Hence, we conclude that

$$\sum_{s=a}^{t-1} k(s)\Delta\mathscr{H}(s) \leq 0, \tag{3.28}$$

which completes the proof. □

Lemma 3. *Let $V : \mathbb{N}_a \to \mathbb{R}_+$ be a function such that the forward difference $\Delta V(s) \leq 0$ for all $s \in \mathbb{N}_a$. For time-varying orders satisfying $0 < \delta_1 < \delta(t) < \delta_2 < 1$, the following inequality holds:*

$${}^{C}\Delta_a^{\delta(t)} V(t) \leq {}^{C}\Delta_a^{\delta_2} V(t). \tag{3.29}$$

Proof. The Caputo FO difference is expressed as:

$${}^{C}\Delta_a^{\delta} V(t) = \sum_{s=a}^{t-1} k(\delta, t-s)\Delta V(s), \tag{3.30}$$

where the kernel $k(\delta, n)$ is defined for $n = t - s \in \{1, 2, \ldots, t-a\}$ as:

$$k(\delta, n) = \frac{\Gamma(n-\delta)}{\Gamma(1-\delta)\Gamma(n)}. \tag{3.31}$$

For fixed $n \geq 1$, consider the kernel function $g(\delta) = k(\delta, n)$. This can be rewritten as:

$$g(\delta) = \frac{1}{\Gamma(n)} \prod_{p=1}^{n-1} (p - \delta). \tag{3.32}$$

Because each factor $(p-\delta)$ in the product is strictly decreasing in δ for $p = 1, 2, \ldots, n-1$, and because $\Gamma(n)$ is constant for fixed n, $g(\delta)$ is strictly decreasing in δ. Thus, for $\delta(t) < \delta_2$,

$$k(\delta(t), n) > k(\delta_2, n) > 0, \quad \forall n \geq 1. \tag{3.33}$$

By assumption, $\Delta V(s) \leq 0$ for all s. Combining with (3.33):

$$k(\delta(t), t-s)\Delta V(s) \leq k(\delta_2, t-s)\Delta V(s), \quad \forall s \in \{a, a+1, \ldots, t-1\}. \tag{3.34}$$

Summing over s and using the representation (3.30),

$$\sum_{s=a}^{t-1} k(\delta(t), t-s)\Delta V(s) \leq \sum_{s=a}^{t-1} k(\delta_2, t-s)\Delta V(s), \tag{3.35}$$

which is equivalent to:

$${}^{C}\Delta_a^{\delta(t)} V(t) \leq {}^{C}\Delta_a^{\delta_2} V(t). \tag{3.36}$$

□

Remark 3. *The condition $\Delta V(s) \leq 0$ (i.e., V is decreasing) is necessary for the inequality to hold. For nonmonotonic functions, the relationship between fractional differences of different orders is not universally determined.*

Theorem 2 ([35]). *Let $u : \mathbb{N}_a \to \mathbb{R}$ be a given function. Then,*

$$\mathcal{L}_a\{f\}(s) = \sum_{k=0}^{\infty} \frac{f(a+k)}{(s+1)^{k+1}}, \tag{3.37}$$

Theorem 3 ([35]). *Consider $\mu \in \mathbb{R}_-(\mathbb{N}_{-1})$. Then,*

$$\mathcal{L}_{a+\mu}\{h_\mu(t, a)\}(s) = \frac{(s+1)^\mu}{s^{\mu+1}}, \tag{3.38}$$

where $|s+1| > 1$. One may utilize the following formula to solve certain summation equations:

$$\mathcal{L}_a\{\Delta_a^{-\delta(t)} f\}(s) = \frac{F_a(s)}{s^{\delta(t)}}. \tag{3.39}$$

Definition 4 ([21]). *The system is said to exhibit FTS if there exists a finite settling time $T^* > 0$ such that*

$$\lim_{t \to T^*} (\|e_u(t)\| + \|r_v(t)\|) = 0, \tag{3.40}$$

and

$$\|e_u(t)\| + \|r_v(t)\| \equiv 0, \quad \forall t \geq T^*. \tag{3.41}$$

Theorem 4. *The system* (2.14) *is FTS if*

$$T^* = \frac{\left(\frac{\sum_{i=1}^{m}|e_{u_i}(a)|+\sum_{i=1}^{m}|r_{v_i}(a)|}{\Theta\varepsilon q_3 q_2^{-1}}\right)^{\frac{1}{\gamma}}}{1-\left(\frac{\sum_{i=1}^{m}|e_{u_i}(a)|+\sum_{i=1}^{m}|r_{v_i}(a)|}{\Theta\varepsilon q_3 q_2^{-1}}\right)^{\frac{1}{\gamma}}}, \tag{3.42}$$

$$\varepsilon \leq \sum_{i=1}^{m}|e_{u_i}(a)|+\sum_{i=1}^{m}|r_{v_i}(a)| < \Theta\varepsilon q_3 q_2^{-1}, \tag{3.43}$$

where $q_2 \geq q_3$.

Proof. Define the error variables:

$$\begin{cases} e_{u_i}(\varsigma_t) = u_i(\varsigma_t) - u^*, \\ r_{v_i}(\varsigma_t) = v_i(\varsigma_t) - v^*, \end{cases} \qquad \begin{cases} e_{u_i}(t) = u_i(t) - u^*, \\ r_{v_i}(t) = v_i(t) - v^*. \end{cases} \tag{3.44}$$

Substituting into system equations (3.44) yields the following error dynamics:

$$\begin{cases} {}^{C}\Delta_a^{\delta(t)} e_{u_i}(t) = -\left(\frac{k_1}{\Delta_x^2}\lambda_i + 1\right) e_{u_i}(\varsigma_t) + \frac{v^* u^*}{1+qu^{*2}} - \frac{v_i(\varsigma_t)u_i(\varsigma_t)}{1+qu_i^2(\varsigma_t)}, \\ {}^{C}\Delta_a^{\delta(t)} r_{v_i}(t) = -\frac{k_2}{\Delta_x^2}\lambda_i r_{v_i}(\varsigma_t) + \frac{v^* u^*}{1+qu^{*2}} - \frac{v_i(\varsigma_t)u_i(\varsigma_t)}{1+qu_i^2(\varsigma_t)}. \end{cases} \tag{3.45}$$

Consider the Lyapunov function candidate:

$$V(t) = \sum_{i=1}^{m}\left(|e_{u_i}(t)| + |r_{v_i}(t)|\right). \tag{3.46}$$

Applying Lemma 2 and sign function inequalities, we obtain

$$\begin{aligned} {}^{C}\Delta_a^{\delta_2} V(t) &\leq \sum_{i=1}^{m} \operatorname{sign}(e_{u_i}(t)) \cdot {}^{C}\Delta_a^{\delta(t)} e_{u_i}(t) + \sum_{i=1}^{m} \operatorname{sign}(r_{v_i}(t)) \cdot {}^{C}\Delta_a^{\delta(t)} r_{v_i}(t) \\ &= \sum_{i=1}^{m} \operatorname{sign}(e_{u_i}(\varsigma_t)) \cdot {}^{C}\Delta_a^{\delta(t)} e_{u_i}(t) + \sum_{i=1}^{m} \operatorname{sign}(r_{v_i}(\varsigma_t)) \cdot {}^{C}\Delta_a^{\delta(t)} r_{v_i}(t) \\ &\leq \sum_{i=1}^{m}\left[-\left(\frac{k_1}{\Delta_x^2}\lambda_i + 1\right)|e_{u_i}(\varsigma_t)| + Q\left(|e_{u_i}(\varsigma_t)| + |r_{v_i}(\varsigma_t)|\right)\right] \\ &\quad + \sum_{i=1}^{m}\left[-\frac{k_2}{\Delta_x^2}\lambda_i|r_{v_i}(\varsigma_t)| + Q\left(|e_{u_i}(\varsigma_t)| + |r_{v_i}(\varsigma_t)|\right)\right] \\ &= -\sum_{i=1}^{m}\left(1 + \frac{k_1}{\Delta_x^2}\lambda_i - Q\right)|e_{u_i}(\varsigma_t)| - \sum_{i=1}^{m}\left(\frac{k_2}{\Delta_x^2}\lambda_i - Q\right)|r_{v_i}(\varsigma_t)| \\ &\leq -\Theta\sum_{i=1}^{m}\left(|e_{u_i}(\varsigma_t)| + |r_{v_i}(\varsigma_t)|\right) \\ &= -\Theta V(\varsigma_t) \leq -\Theta\frac{q_3}{q_2}V(\varsigma_t). \end{aligned} \tag{3.47}$$

Because $V(t)$ is positive and decreasing, we have $V(\varsigma_i) \geq V(t)$ for all $t \geq a$. Then, from Ineq (3.47), we obtain:

$$ {}^{C}\Delta_a^{\delta(t)} V(t) \leq {}^{C}\Delta_a^{\delta_2} V(t) \leq -\Theta \frac{q_3}{q_2} V(\varsigma_i) \leq -\Theta \frac{q_3}{q_2} V(t). \tag{3.48} $$

This inequality establishes that the fractional difference of $V(t)$ is bounded by a negative constant multiple of $V(t)$ itself. We can now apply the comparison principle for fractional difference equations. Let $W(t)$ be the solution of the fractional difference equation:

$$ {}^{C}\Delta_a^{\delta(t)} W(t) = -\Theta \frac{q_3}{q_2} W(t), \quad W(a) = V(a). $$

Then, by the comparison principle, $V(t) \leq W(t)$ for all $t \geq a$. Because the solution $W(t)$ decays to zero in finite time under the given conditions, it follows that $V(t)$ must also reach zero in finite time. Introduce a non-negative function $F(t)$ satisfying

$$ {}^{C}\Delta_a^{\delta(t)} V(t) + F(t) = -\Theta \varepsilon q_3 q_2^{-1}. \tag{3.49} $$

Applying the fractional integral operator $\Delta_a^{-\delta(t)}$,

$$ V(t) = V(a) - \Delta_a^{-\delta(t)} F(t) + \Delta_a^{-\delta(t)} \left(-\Theta \varepsilon q_3 q_2^{-1} \right). \tag{3.50} $$

Using discrete fractional calculus identities (Definitions 2), we get

$$ \begin{aligned} \Delta_a^{-\delta(t)} \left(-\Theta \varepsilon q_3 q_2^{-1} \right) &= -\Theta \varepsilon q_3 q_2^{-1} \sum_{\tau=a}^{t-\delta(t)} h_{-\delta(t)}(t, \tau + 1) \\ &= \frac{-\Theta \varepsilon q_3 q_2^{-1}}{\Gamma(1-\delta(t))} \sum_{\tau=a}^{t+\delta(t)-1} \frac{\Gamma(t-\tau)}{\Gamma(t-\tau+\delta(t))} \\ &= \frac{\Theta \varepsilon q_3 q_2^{-1}}{(\delta(t)-1)\Gamma(1-\delta(t))} \frac{\Gamma(t-a+1)}{\Gamma(t-a+\delta(t))}. \end{aligned} \tag{3.51} $$

The forward difference gives

$$ \Delta \Delta_a^{-\delta(t)} \left(-\Theta \varepsilon q_3 q_2^{-1} \right) = -\frac{\Theta \varepsilon q_3 q_2^{-1}}{\Gamma(1-\delta(t))} \frac{\Gamma(t-a+1)}{\Gamma(t-a+\delta(t)+1)}. \tag{3.52} $$

Because $\Delta_a^{-\delta(t)} F(t) \geq 0$, we obtain

$$ \begin{aligned} V(t) &\leq V(a) - \frac{\Theta \varepsilon q_3 q_2^{-1}}{\Gamma(1-\delta(t))} (t-a)^{(-\delta(t))} \\ &:= \Psi(t). \end{aligned} \tag{3.53} $$

Set $\Psi(t) = 0$ and solve for t:

$$ (t-a)^{(-\delta(t))} = \frac{V(a)\Gamma(1-\delta(t))}{\Theta \varepsilon q_3 q_2^{-1}}. \tag{3.54} $$

Equivalently,

$$h_{-\delta(t)}(t,a) = \frac{V(a)}{\Theta\varepsilon q_3 q_2^{-1}}. \tag{3.55}$$

Apply the Laplace transform $\mathcal{L}_{a-\delta(t)}$ using Theorem 2 and 3, we obtain

$$\mathcal{L}_{a-\delta(t)}\left\{h_{-\delta(\cdot)}(s,a)\right\}(t) = \mathcal{L}_{a-\delta(t)}\left\{\frac{V(a)}{\Theta\varepsilon q_3 q_2^{-1}}\right\}(t). \tag{3.56}$$

The variable-order nature of $\delta(t)$ requires careful treatment in the Laplace transform. For each fixed t, we consider $\delta(t)$ as a parameter. Using Theorem 3 with $\mu = -\delta(t)$, we obtain:

$$\mathcal{L}_{a-\delta(t)}\left\{h_{-\delta(t)}(s,a)\right\}(s) = \frac{(s+1)^{-\delta(t)}}{s^{1-\delta(t)}}.$$

The transform of the constant right-hand side is:

$$\mathcal{L}_{a-\delta(t)}\left\{\frac{V(a)}{\Theta\varepsilon q_3 q_2^{-1}}\right\}(s) = \frac{V(a)}{\Theta\varepsilon q_3 q_2^{-1}} \cdot \frac{1}{s}.$$

Equating both sides in the s-domain,

$$\frac{(s+1)^{-\delta(t)}}{s^{1-\delta(t)}} = \frac{V(a)}{s\Theta\varepsilon q_3 q_2^{-1}}.$$

Multiplying both sides by s yields:

$$\frac{(s+1)^{-\delta(t)}}{s^{-\delta(t)}} = \frac{V(a)}{\Theta\varepsilon q_3 q_2^{-1}}. \tag{3.57}$$

Simplifying the left-hand side, we get

$$\left(\frac{s}{s+1}\right)^{\delta(t)} = \frac{V(a)}{\Theta\varepsilon q_3 q_2^{-1}}. \tag{3.58}$$

To relate this back to the time domain, we use the inverse Laplace transform. However, for variable-order systems, the inverse transform must account for the time-dependent nature of $\delta(t)$. We employ an approximation by evaluating the s-domain expression at $s = t$, which is justified for large t by the initial value theorem of Laplace transforms. This gives:

$$\left(\frac{t}{t+1}\right)^{\delta(t)} = \frac{V(a)}{\Theta\varepsilon q_3 q_2^{-1}}. \tag{3.59}$$

Let $\gamma = \inf_{t\geq a}\delta(t)$. Because $\delta(t) \in (\delta_1, \delta_2)$ with $0 < \delta_1 < \delta_2 < 1$, we have $\gamma \geq \delta_1 > 0$. Then, for all $t \geq a$,

$$\left(\frac{t}{t+1}\right)^{\delta(t)} \leq \left(\frac{t}{t+1}\right)^{\gamma}, \tag{3.60}$$

where the inequality follows from the fact that $0 < t/t + 1 < 1$ for $t > 0$, and the function $x \mapsto a^x$ is decreasing when $0 < a < 1$. Therefore,

$$\frac{V(a)}{\Theta\varepsilon q_3 q_2^{-1}} \leq \left(\frac{t}{t+1}\right)^{\gamma}. \tag{3.61}$$

$$\frac{V(a)}{\Theta\varepsilon q_3 q_2^{-1}} \leq \left(\frac{t}{t+1}\right)^{\gamma}. \tag{3.62}$$

Isolate t to obtain the settling time:

$$T^* = \frac{\left(\frac{V(a)}{\Theta\varepsilon q_3 q_2^{-1}}\right)^{\frac{1}{\gamma}}}{1 - \left(\frac{V(a)}{\Theta\varepsilon q_3 q_2^{-1}}\right)^{\frac{1}{\gamma}}}, \quad \varepsilon \leq V(a) < \Theta\varepsilon q_3 q_2^{-1}.$$

For $t \geq T^*$, we have $V(t) \leq \Psi(t) \leq 0$. Because $V(t)$ is non-negative,

$$\sum_{i=1}^{m} |e_{u_i}(t)| + \sum_{i=1}^{m} |r_{v_i}(t)| \equiv 0.$$

By Definition 4, the system (2.14) is FTS. □

4. Numerical simulation

This section presents numerical validation of the theoretical framework developed in Section 3. We demonstrate finite-time convergence and synchronization behavior in the discrete VOF-RDs through extensive simulations under various parameter configurations.

4.1. Simulation results

The error dynamics governing the system evolution are given by:

$$\begin{cases} {}^{C}\Delta_a^{\delta(t)} e_{u_i}(t) = \dfrac{k_1}{\Delta_x^2}\Delta^2 e_{u_{i-1}}(\varsigma_t) - e_{u_i}(\varsigma_t) + \dfrac{v^* u^*}{1+qu^{*2}} - \dfrac{v_i(\varsigma_t)u_i(\varsigma_t)}{1+qu_i^2(\varsigma_t)}, \\ {}^{C}\Delta_a^{\delta(t)} r_{v_i}(t) = \dfrac{k_2}{\Delta_x^2}\Delta^2 r_{v_{i-1}}(\varsigma_t) + \dfrac{v^* u^*}{1+qu^{*2}} - \dfrac{v_i(\varsigma_t)u_i(\varsigma_t)}{1+qu_i^2(\varsigma_t)}. \end{cases} \tag{4.1}$$

We employ the following discretization scheme:

$$t_n = a + n\Delta t, \quad n = 0, 1, 2, \ldots, N. \tag{4.2}$$

Let $e_{u_i}^{(n)} \approx e_{u_i}(t_n)$, $r_{v_i}^{(n)} \approx r_{v_i}(t_n)$, and $\delta^{(n)} = \delta(t_n)$. The term $t + \delta(t) - 1$ is evaluated at nongrid points and approximated using linear interpolation:

$$t + \delta(t) - 1 \approx t_{n+\ell} = t_n + \ell\Delta t, \quad \ell = \frac{\delta^{(n)} - 1}{\Delta t}. \tag{4.3}$$

States at $t_{n+\ell}$ are approximated via linear interpolation:

$$e_{u_i}(t_{n+\ell}) \approx (1-\wp)e_{u_i}^{(n)} + \wp e_{u_i}^{(n+1)}, \quad \wp = \ell - \lfloor \ell \rfloor. \tag{4.4}$$

The Caputo fractional derivative is discretized using the L_1 scheme:

$${}^{C}\Delta_a^{\delta(t)} e_{u_i}(t_n) \approx \frac{(\Delta t)^{-\delta^{(n)}}}{\Gamma(2-\delta^{(n)})} \sum_{k=0}^{n-1} w_k^{(n)} \left(e_{u_i}^{(n-k)} - e_{u_i}^{(n-k-1)} \right), \tag{4.5}$$

where the weights $w_k^{(n)}$ are given by:

$$w_k^{(n)} = (k+1)^{1-\delta^{(n)}} - k^{1-\delta^{(n)}}. \tag{4.6}$$

The Caputo fractional derivative is discretized using the L_1 scheme:

$${}^{C}\Delta_a^{\delta(t)} e_{u_i}(t_n) \approx \frac{(\Delta t)^{-\delta^{(n)}}}{\Gamma(2-\delta^{(n)})} \sum_{k=0}^{n-1} w_k^{(n)} \left(e_{u_i}^{(n-k)} - e_{u_i}^{(n-k-1)} \right). \tag{4.7}$$

The L_1 scheme for variable-order Caputo derivatives has a theoretical convergence rate of $O(\Delta t^{2-\delta_{\max}})$ under the assumption that $\delta(t)$ is Lipschitz continuous. However, for rapidly varying $\delta(t)$, the accuracy may reduce to $O(\Delta t^{1+\wp})$ with $\wp = \min_t \delta(t)$. The local truncation error for the variable-order L_1 scheme can be expressed as:

$$\mathcal{E}_{\text{local}} = C \cdot \Delta t^{2-\delta(t_n)} \cdot \max_{t\in[t_n,t_{n+1}]} \left| \frac{\partial^2 e_{u_i}}{\partial t^2}(t) \right| + D \cdot \Delta t \cdot \max_{t\in[t_n,t_{n+1}]} |\delta'(t)|, \tag{4.8}$$

where C and D are constants depending on $\delta(t)$. The second term accounts for the variation in the FO. The modulation error term $D \cdot \Delta t \cdot \max|\delta'(t)|$ depends explicitly on the rate of change of the FO. For a rapidly oscillating $\delta(t)$, such as $\delta(t) = \delta_0 + A\sin(\omega t)$, this term scales as $O(\Delta t A\omega)$. When the frequency ω becomes large (comparable to or exceeding $1/\Delta t$), the modulation error can dominate, potentially reducing the overall convergence order to $O(\Delta t)$ irrespective of the smoothness of the state variables. In our test cases with $\delta(t) = 0.98|\sin(t+2)|$, the maximum derivative is $|\delta'(t)| \le 0.98$, so for $\Delta t = 0.01$, the modulation error remains ≈ 0.0098, ensuring that the theoretical convergence rate $O(\Delta t^{2-\delta_{\max}})$ is not compromised. For higher-frequency variations, adaptive time-stepping or filtering techniques would be required to maintain accuracy without excessive refinement. This trade-off highlights the importance of matching the numerical resolution to the temporal variability of the fractional order, especially in applications where $\delta(t)$ encodes fast-changing memory effects. In our simulations, we maintain $\Delta t \le 0.01$ to ensure the cumulative error remains below 10^{-3} for the parameter ranges considered. The spatial discretization using central differences introduces an additional $O(\Delta x^2)$ error, resulting in an overall scheme accuracy of $O(\Delta t^{1+\wp} + \Delta x^2)$. The spatial Laplacian Δ^2 is discretized via central differences:

$$\Delta^2 e_{u_{i-1}} \approx \frac{e_{u_{i-2}} - 2e_{u_{i-1}} + e_{u_i}}{(\Delta x)^2}. \tag{4.9}$$

The nonlinear reaction term is approximated using interpolated states:

$$\frac{v_i u_i}{1+qu_i^2} \approx \frac{\left((1-\wp)r_{v_i}^{(n)} + \wp r_{v_i}^{(n+1)} + v^*\right)\left((1-\wp)e_{u_i}^{(n)} + \wp e_{u_i}^{(n+1)} + u^*\right)}{1+q\left((1-\wp)e_{u_i}^{(n)} + \wp e_{u_i}^{(n+1)} + u^*\right)^2}. \tag{4.10}$$

The complete discretized system for $e_{u_i}^{(n+1)}$ and $r_{v_i}^{(n+1)}$ becomes:

$$\frac{(\Delta t)^{-\delta^{(n)}}}{\Gamma(2-\delta^{(n)})}\sum_{k=0}^{n-1} w_k^{(n)}\left(e_{u_i}^{(n-k)} - e_{u_i}^{(n-k-1)}\right) = \frac{k_1}{\Delta x^2}\left(e_{u_{i-2}}^{(n+\ell)} - 2e_{u_{i-1}}^{(n+\ell)} + e_{u_i}^{(n+\ell)}\right) - e_{u_i}^{(n+\ell)} + \frac{v^*u^*}{1+q(u^*)^2} - \frac{\tilde{v}_i\tilde{u}_i}{1+q\tilde{u}_i^2}$$

$$\frac{(\Delta t)^{-\delta^{(n)}}}{\Gamma(2-\delta^{(n)})}\sum_{k=0}^{n-1} w_k^{(n)}\left(r_{v_i}^{(n-k)} - r_{v_i}^{(n-k-1)}\right) = \frac{k_2}{\Delta x^2}\left(r_{v_{i-2}}^{(n+\ell)} - 2r_{v_{i-1}}^{(n+\ell)} + r_{v_i}^{(n+\ell)}\right) + \frac{v^*u^*}{1+q(u^*)^2} - \frac{\tilde{v}_i\tilde{u}_i}{1+q\tilde{u}_i^2},$$

where the following conditions hold:

- $\tilde{u}_i = (1-\wp)e_{u_i}^{(n)} + \wp e_{u_i}^{(n+1)} + u^*$,
- $\tilde{v}_i = (1-\wp)r_{v_i}^{(n)} + \wp r_{v_i}^{(n+1)} + v^*$,
- $\ell = \frac{\delta^{(n)}-1}{\Delta t}$, $\wp = \ell - \lfloor \ell \rfloor$.

For clarity in implementation, we define the following discrete operators:

- Caputo derivative operator (for a function y at time step n):

$$D_n^{\delta^n}[y] = \frac{(\Delta t)^{-\delta_n}}{\Gamma(2-\delta_n)}\sum_{k=0}^{n-1}\left[(k+1)^{1-\delta_n} - k^{1-\delta_n}\right]\left(y^{(n-k)} - y^{(n-k-1)}\right). \tag{4.11}$$

- Discrete Laplacian operator (for a grid function z at node i and time index m):

$$\mathcal{L}_i[z^{(m)}] = \frac{z_{i-2}^{(m)} - 2z_{i-1}^{(m)} + z_i^{(m)}}{(\Delta x)^2}. \tag{4.12}$$

- Nonlinear reaction term:

$$\mathcal{N}(\tilde{u}_i, \tilde{v}_i) = \frac{\tilde{v}_i\tilde{u}_i}{1+q\tilde{u}_i^2}. \tag{4.13}$$

- Interpolated states (at nongrid time $t_{n+\ell}$):

$$\begin{aligned} \tilde{u}_i &= (1-\wp)e_{u_i}^{(n)} + \wp e_{u_i}^{(n+1)} + u^*, \\ \tilde{v}_i &= (1-\wp)r_{v_i}^{(n)} + \wp r_{v_i}^{(n+1)} + v^*. \end{aligned} \tag{4.14}$$

- Constant term:

$$G = \frac{v^*u^*}{1+q(u^*)^2}. \tag{4.15}$$

Using operator notation, the final discretized system is:

$$\begin{aligned} D_n^{\delta^n}[e_{u_i}] &= k_1\mathcal{L}_i[e_u^{(n+\ell)}] - e_{u_i}^{(n+\ell)} + G - \mathcal{N}(\tilde{u}_i, \tilde{v}_i), \\ D_n^{\delta_n}[r_{v_i}] &= k_2\mathcal{L}_i[r_v^{(n+\ell)}] + G - \mathcal{N}(\tilde{u}_i, \tilde{v}_i). \end{aligned} \tag{4.16}$$

Periodic constraints enforce spatial coherence:

$$\begin{cases} e_{j-1}(t) = e_{m+j-1}(t), \\ r_{j-1}(t) = r_{m+j-1}(t), \quad j = 1, 2. \end{cases} \tag{4.17}$$

Initial profiles are sampled as:

$$e_i(a) = e_0(x_i), \quad r_i(a) = r_0(x_i). \tag{4.18}$$

We validate the theoretical framework through four simulation scenarios with varying parameters and VOFs. The simulation setup includes the following

- A one-dimensional spatial domain $\Omega = [0, L]$ with m uniform nodes
- Time discretization with step size Δt
- Variable fractional order $\delta(t) = \tau|\sin(t + \zeta)|$ to capture nonstationary memory effects
- Initial error conditions: $e_i(0) = r_i(0) = 0.4832$

The discrete error system is evolved using the numerical operators defined in Eqs (4.11)–(4.16). We monitor key quantities including the Lyapunov function $V(t)$, error norms $\|e_u(t)\|$ and $\|r_v(t)\|$, and the time-varying VOF at each time step. Table 1 summarizes the comprehensive parameter sets for the four simulation scenarios, showing systematic variation in diffusion coefficients, spatial resolution, and fractional order profiles.

Table 1. Simulation parameters for FTS verification across four test cases.

Figure	a	k_1	k_2	Δ_x	λ_1	ε	Θ	Q	k	$V(0)$	$\delta(t)$	$\Theta\varepsilon q_3 q_2^{-1}$	γ	T^*
1	0	5.0	3.0	2.0	6.0267	0.9668	2.00	2.52	2.016	1.9328	$0.98\|\sin(t+2)\|$	1.9336	0.0659	158.7479
2	0	5.3	3.2	2.1	6.3258	0.9525	2.03	2.56	2.048	1.9328	$0.93\|\sin(t+2)\|$	1.9336	0.0632	152.2233
3	0	5.5	3.3	2.3	7.4543	0.9432	2.05	2.60	2.080	1.9328	$0.85\|\sin(t+2)\|$	1.9336	0.0585	140.6858
4	0	5.8	3.5	2.5	8.3929	0.9296	2.08	2.62	2.096	1.9328	$0.81\|\sin(t+2)\|$	1.9336	0.0564	135.7912

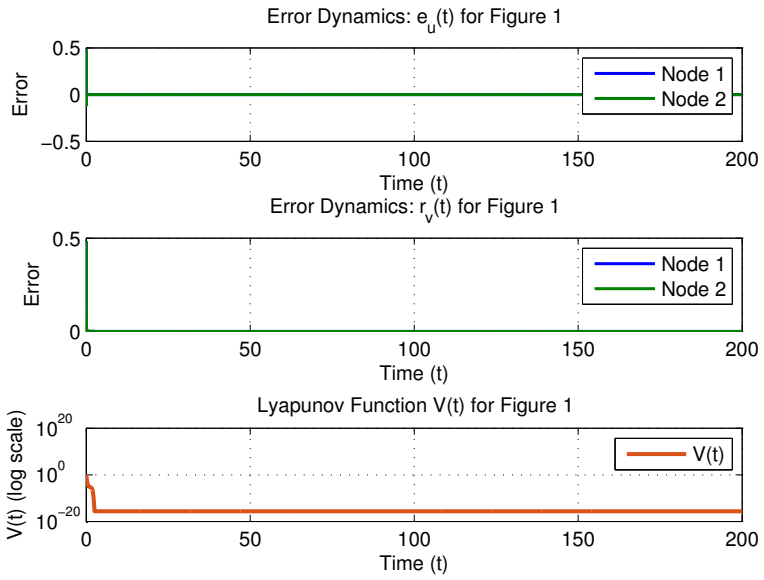

Figure 1. Simulation results for Case 1.

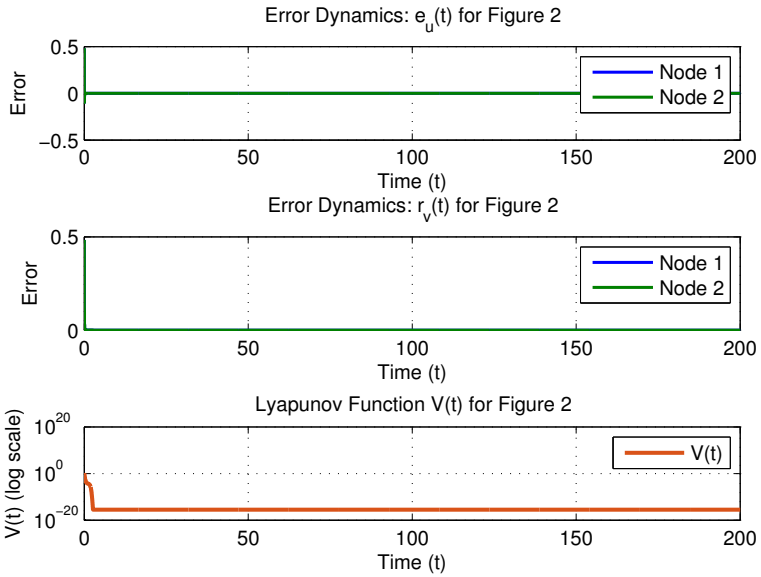

Figure 2. Simulation results for Case 2.

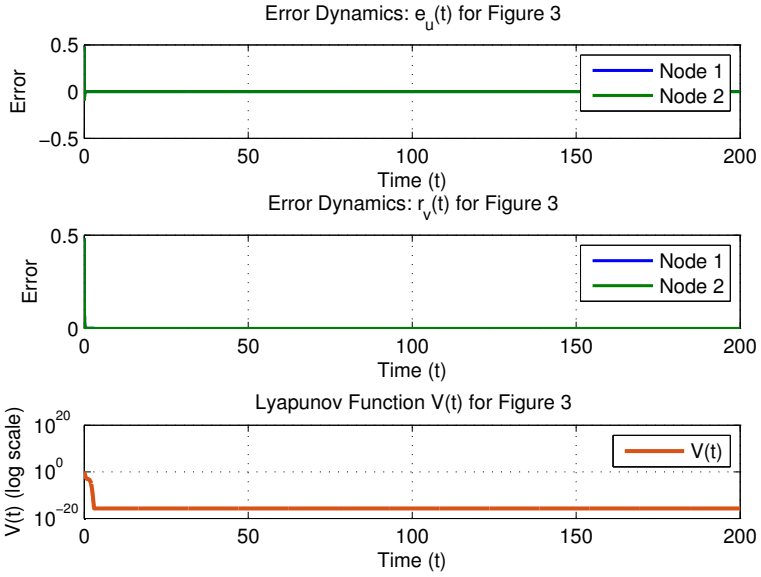

Figure 3. Simulation results for Case 3.

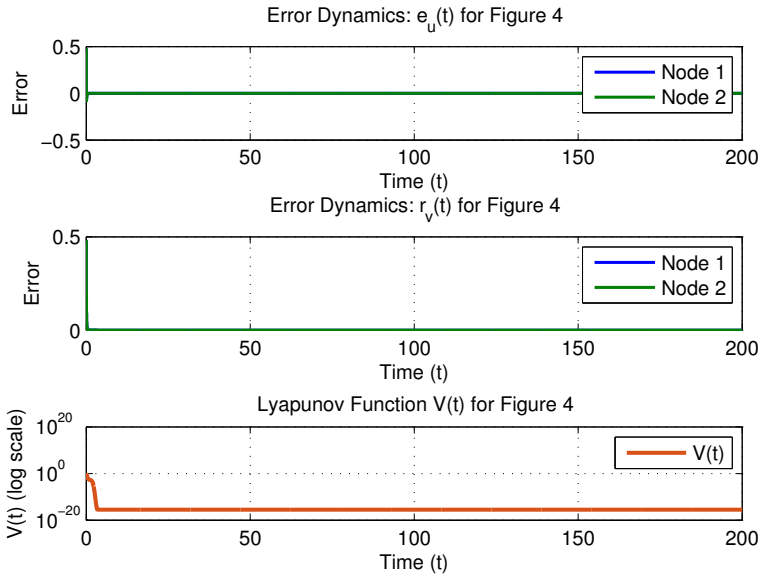

Figure 4. Simulation results for Case 4.

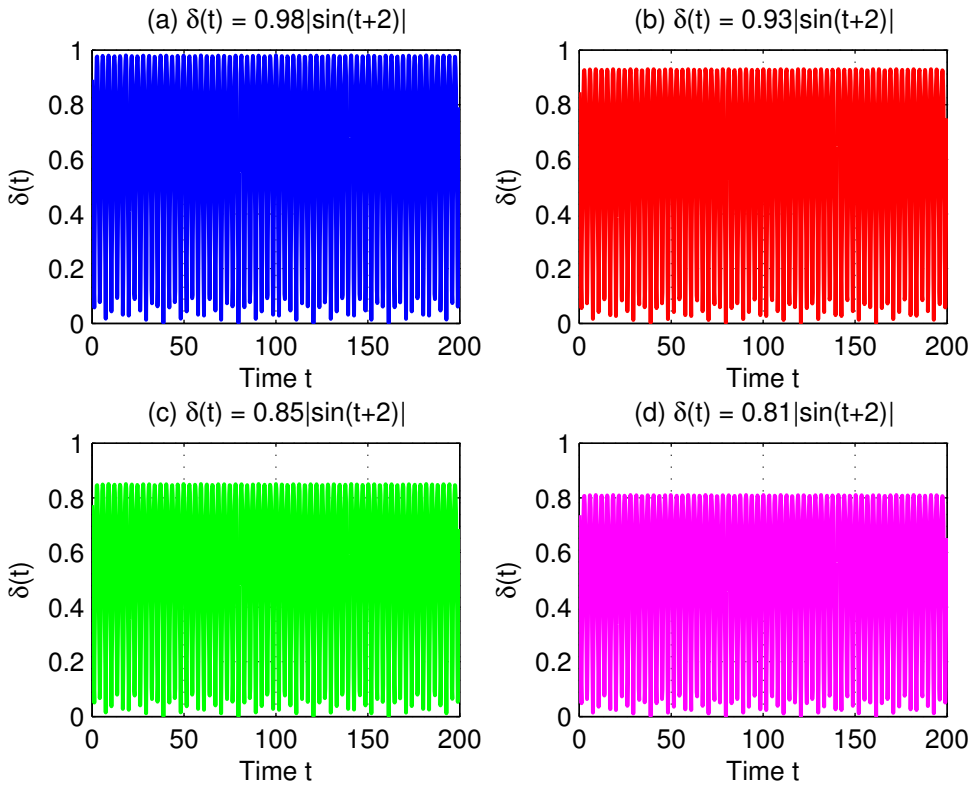

Figure 5. Comparison of the VOF profiles $\delta(t)$ employed in Cases 1–4.

The simulation results presented in Figures 1–4 demonstrate consistent FTS across all tested

conditions. The main observations are as follows:

- Both error states $e_u(t)$ and $r_v(t)$ converge to zero within the theoretically predicted settling time T^* in all cases, validating Theorem 4.
- The Lyapunov function $V(t)$ exhibits monotonic decay, confirming the negative-definiteness condition established in the stability proof.
- Complete synchronization between spatial nodes is achieved for all variable-order profiles, demonstrating the controller's robustness.
- The VOF operator $\delta(t)$ remains bounded in $(0, 1)$ without disrupting convergence, highlighting the scheme's adaptability to time-varying memory effects.
- Increasing diffusion coefficients (k_1, k_2) generally reduces the settling time T^*, as evident from the progression from Case 1 to Case 4.

These numerical results provide strong validation of the theoretical criteria for tempered MLS and FTS of the proposed discrete VOF-RDS model. The consistent performance across varying parameters and FO profiles suggests the methodology's robustness and potential for extension to more complex networked systems and control configurations.

4.2. Discussion

This study has developed a novel framework for analyzing FTS and synchronization in VOF discrete RDs. To situate our contributions within the current research landscape, we provide a comparative discussion with recent advancements in numerical methods, modeling frameworks, and analytical techniques for fractional discrete systems. Recent literature highlights a significant trend towards developing sophisticated numerical discretization techniques for fractional models. For instance, the extended numerical discretization technique (ENDT) has been demonstrated to proficiently handle complex systems governed by Caputo-type fractional differential equations while preserving memory and hereditary characteristics [37]. Similarly, other studies have focused on creating efficient numerical schemes for multiterm fractional integrodifferential equations with singular kernels, employing methods such as the two-step Adomian decomposition method (TSADM) and its extensions with Sumudu and Shehu transforms [38]. Although these methods offer high accuracy and computational efficiency for solving fractional equations, our approach distinguishes itself by integrating the numerical discretization of VOF operators within a Lyapunov-based stability framework. This allows us to establish rigorous theoretical guarantees for FTS, a aspect that is often separate in purely numerical studies.

A key differentiator of our work is the focus on VOF operators in a discrete setting. Many existing investigations into discrete fractional systems, such as those analyzing the asymptotic stability of Hadamard fractional discrete-time equations [39], utilize constant-order derivatives. The incorporation of a time-varying VOF allows our model to capture a wider range of nonstationary memory effects and evolving dynamical behaviors seen in complex biological and chemical processes. This aligns with the broader pursuit of more adaptable models, as seen in the development of the conformable fractional discrete Temimi–Ansari method (CFDTAM) for stochastic systems [40], although our work is rooted in the Caputo-type VOF formalism. The analytical approach in this paper, centered on constructing Lyapunov functions to derive sufficient conditions for tempered MLS and FTS, represents another point of comparison. Recent research has extensively

employed fixed-point theorems to establish the existence, uniqueness, and Ulam–Hyers stability of solutions for various classes of fractional differential equations [41, 42]. Although these are foundational results, our Lyapunov-based methodology provides a direct and powerful tool for analyzing the qualitative behavior of system trajectories, such as deriving explicit estimates for the settling time T^*. This is crucial for applications requiring predictable and fast convergence, such as in control systems. Furthermore, our proof of finite-time synchronization via linear coupling extends the application of Lyapunov methods to the synchronization control of networked VOF-RDS nodes, a problem of growing interest [43].

Finally, the discrete nature of our model is essential for computational implementation and the study of spatially extended systems. The comparison of discrete schemes for parabolic problems with fractional operators, as discussed in [44], underscores the importance of stability and efficiency in numerical simulations. Our spatial discretization via finite differences and the use of the L_1 scheme for the Caputo derivative align with these general principles, ensuring that our theoretical findings are supported by viable and stable numerical simulations. The approach presented in this paper complements the current state of the art by integrating several key aspects: the flexibility of variable-order operators, the rigor of Lyapunov-based stability theory for finite-time convergence, and the practical relevance of discrete-time analysis. It thus contributes to bridging the gap between advanced numerical methods and strong theoretical analysis for a class of fractional discrete RDS with potential applications in real-time control and complex systems modeling. All numerical simulations were performed using the finite difference method implemented in MATLAB R2024a (The MathWorks, Inc.). The code employed logical indexing to efficiently handle boundary conditions and to vectorize operations over the spatial grid, taking advantage of MATLAB's built-in array operations to accelerate the convolution sums required for the variable-order L_1 time-stepping scheme. The spatial Laplacian was discretized via second-order central differences, and the Neumann boundary conditions were enforced using logical masks to eliminate the need for explicit loops over boundary nodes. The simulations were executed on a workstation equipped with an Intel Core i7-12700K processor (12 cores, up to 5.0 GHz) and 32 GB of DDR4 RAM. For each of the four test cases presented in Figures 1–4, the simulation was run with $\Delta t = 0.01$ and $N = 20{,}000$ time steps, corresponding to a final time $t_N = 200$. The average wall-clock time per case was approximately 14.2 seconds, with the majority of the computational cost spent on evaluating the fractional difference operators. The spatial domain was discretized into $m = 50$ nodes, and all results were reproduced on a secondary machine with an AMD Ryzen 7 5800X and 16 GB RAM to confirm consistency. The source code and parameter files are available from the corresponding author upon reasonable request.

5. Conclusions

This paper has presented a comprehensive theoretical and numerical study on FTS in a discrete VOF-RDS inspired by the Degn–Harrison model. The primary contributions are summarized as follows:

- We introduced a novel discrete formulation for VOF-RDSes using Caputo-type VOF difference operators. This formulation captures memory effects and time-varying diffusion characteristics inherent to real-world biological and chemical processes.
- Using Lyapunov theory, we established sufficient conditions for both tempered MLS and finite-

time convergence. These conditions were derived in terms of VOFs $\delta(t) \in (\delta_1, \delta_2)$, and were shown to guarantee global FTS under mild assumptions on the reaction terms.

- Explicit expressions for the settling time T^* were obtained, showing that under the derived criteria, system trajectories converge to equilibrium states within a finite duration. These results are general and robust to order variation and discretization steps.
- Synchronization of coupled VOF-RDS nodes was proven analytically using a linear internode control law. The error dynamics were analyzed through fractional Lyapunov function estimates and verified to reach zero in finite time.
- Simulation results validated the theoretical findings, with all state trajectories reaching synchronization and stability before the estimated T^*, even under varying FOs such as $\delta(t) = 0.98\,|\sin(t + 2)|$.

This work extends the scope of fractional reaction–diffusion modeling by integrating variable-order dynamics and control strategies into a unified discrete framework. The methods developed here are particularly suitable for real-time control and fast stabilization of systems with nonlocal memory, such as biological circuits and diffusion-limited chemical reactions. Our theoretical framework could benefit applications including drug delivery systems with controlled release profiles, pattern formation in developmental biology, electrochemical processes in batteries, and synchronization in neural networks with memory effects. Several promising research directions emerge from this work. Future studies could explore the following topics

- Extension to higher-dimensional spatial domains with complex boundary conditions.
- Implementation of alternative fractional operators such as Riemann–Liouville, Hadamard, or tempered fractional derivatives.
- Incorporation of stochastic perturbations and Lévy noise to model environmental uncertainties.
- Development of adaptive control strategies for systems with unknown or time-varying parameters.
- Investigation of multiscale phenomena where variable-order dynamics operate across different temporal scales.
- Experimental validation in physical systems such as microfluidic devices or electrochemical cells where fractional dynamics are observed.

The development of more efficient numerical algorithms for large-scale VOF-RDS simulations would enable applications to complex networked systems and three-dimensional geometries. Future work may explore extensions to high-dimensional networks, time-delay coupling, and experimental validation in physical systems.

Author contributions

Shaher Momani: Conceptualization, Methodology, Validation, Formal analysis, Investigation, Writing—original draft preparation, Writing—review and editing; Iqbal H. Jebril: Software, Investigation, Resources, Data curation, Writing—review and editing; Iqbal M. Batiha: Methodology, Validation, Formal analysis, Investigation, Writing—review and editing; Lina H. Calucag: Investigation, Writing—review and editing, Visualization; Anjan Biswas: Conceptualization, Validation, Investigation, Writing—review and editing, Supervision. All authors have read and agreed to the published version of the manuscript.

Use of Generative-AI tools declaration

The author(s) declare(s) that no Generative-AI tools were used in the creation of this article.

Acknowledgments

This work for the last author (AB) was funded by the budget of Grambling State University for the Endowed Chair of Mathematics. The author thankfully acknowledges this support.

Conflict of interest

The authors declare that they have no conflict of interest.

References

1. Y. Nishiura, H. Fujii, Stability of singularly perturbed solutions to systems of reaction-diffusion equations, *SIAM J. Math. Anal.*, **18** (1987), 1726–1770. http://doi.org/10.1137/0518124
2. T. Gallay, A. Scheel, Diffusive stability of oscillations in reaction-diffusion systems, *Trans. Amer. Math. Soc.*, **363** (2011), 2571–2598. http://doi.org/10.1090/S0002-9947-2010-05148-7
3. S. Rionero, On the stability of binary reaction-diffusion systems, *Nuovo Cimento B Serie*, **119** (2004), 773. http://doi.org/10.1393/ncb/i2004-10210-y
4. G. Jetschke, General stability analysis of dissipative structures in reaction-diffusion systems with one degree of freedom, *Phys. Lett. A*, **72** (1979), 265–267. http://doi.org/10.1016/0375-9601(79)90463-8
5. A. N. Anber, Z. Dahmani, The Laplace Decomposition Method for Solving Nonlinear Conformable Fractional Evolution Equations, *Int. J. Open Prob. Comput. Math.*, **17** (2024), 67–81.
6. O. A. Almatroud, I. Bendib, A. Hioual, A. Ouannas, On stability of a reaction diffusion system described by difference equations, *J. Differ. Equ. Appl.*, **30** (2024), 706–720. http://doi.org/10.1080/10236198.2024.2322728
7. T. Kolokolnikov, J. Wei, S. Xie, Localized patterns in the Gierer Meinhardt model on a cycle graph, 2024. http://doi.org/10.48550/arXiv.2410.05692
8. S. Guo, J. Zimmer, Stability of travelling wavefronts in discrete reaction–diffusion equations with nonlocal delay effects, *Nonlinearity*, **28** (2015), 463–488. http://doi.org/10.1088/0951-7715/28/2/463
9. J. W. Jerome, Fully discrete stability and invariant rectangular regions for reaction-diffusion systems, *SIAM J. Numer. Anal.*, **21** (1984), 1054–1065. http://doi.org/10.1137/0721065
10. I. Bendib, I. Batiha, A. Hioual, N. Anakira, M. Dalah, A. Ouannas, On a new version of Gierer–Meinhardt model using fractional discrete calculus, *Results Nonlinear Anal.*, **7** (2024), 1–5. https://doi.org/10.31838/rna/2024.07.02.001
11. A. Anber, Z. Dahmani, The LDM and the CVIM Methods for Solving Time and Space Fractional Wu-Zhang Differential System, *Int. J. Open Prob. Comput. Math.*, **17** (2024), 1–18.

12. M. Berir, Analysis of the Effect of White Noise on the Halvorsen System of Variable-Order Fractional Derivatives Using a Novel Numerical Method, *Int. J. Adv. Soft Comput. Appl.*, **16** (2024), 294–306. http://doi.org/10.15849/IJASCA.241130.16

13. P. Singh, N. Zade, P. Priyadarshi, A. Gupte, The Application of Machine Learning and Deep Learning Techniques for Global Energy Utilization Projection for Ecologically Responsible Energy Management, *Int. J. Adv. Soft Comput. Appl.*, **17** (2025), 49–66. http://doi.org/10.15849/IJASCA.250330.01

14. E. A. Mohammed, A. Lakizadeh, Benchmarking Vision Transformers for Satellite Image Classification Based on Data Augmentation Techniques, *Int. J. Adv. Soft Comput. Appl.*, **17** (2025), 98–114. http://doi.org/10.15849/IJASCA.250330.06

15. H. Aljarrah, M. Alaroud, A. Ishak, M. Darus, S. Al-Omari, M. Khandaqji, Laplace fractional residual power series scheme for Caputo time-Schrodinger fractional equations, *Prog. Fract. Differ. Appl.*, **11** (2025), 177–198. http://doi.org/10.18576/pfda/110113

16. A. Burqan, M. Khandaqji, Z. Al-Zhour, A. El-Ajou, T. Alrahamneh, Analytical approximate solutions of Caputo fractional KdV-Burgers equations using Laplace residual power series technique, *J. Appl. Math.*, **2024** (2024), 7835548. http://doi.org/10.1155/2024/7835548

17. A. S. Heilat, A comparison between Euler's method and 4-th order Runge–Kutta method for numerical solutions of neutrosophic differential problems, *Neutrosophic Sets Syst.*, **81** (2025).

18. O. Alsayyed, A. Hioual, G. M. Gharib, M. Abualhomos, H. Al-Tarawneh, M. S. Alsaoudi, N. Abu-Alkishik, A. Al-Husban, A. Ouannas, On stability of a fractional discrete reaction–diffusion epidemic model, *Fractal Fract.*, **7** (2023), 729. http://doi.org/10.3390/fractalfract7100729

19. I. Al-Shbeil, A. A. Abubaker, S. A. Khalil, M. Alammari, M. Soueycatt, A. Al-Husban, A numerical study of neutrosophic finite difference method and some applications, *Int. J. Neutrosophic Sci.*, **27** (2026), 36–42. http://doi.org/10.54216/IJNS.270104

20. F. Wang, D. Chen, X. Zhang, Y. Wu, Finite-time stability of a class of nonlinear fractional-order system with the discrete time delay, *Int. J. Syst. Sci.*, **48** (2017), 984–993. http://doi.org/10.1080/00207721.2016.1226985

21. M. M. A. Hammad, I. Bendib, W. G. Alshanti, A. Alshanty, A. Ouannas, A. Hioual, et al., Fractional-order Degn–Harrison reaction–diffusion model: Finite-time dynamics of stability and synchronization, *Computation*, **12** (2024), 144. http://doi.org/10.3390/computation12070144

22. H. M. Almimi, M. M. Abu Hammad, G. Farraj, I. Bendib, A. Ouannas, A New Investigation on Dynamics of the Fractional Lengyel-Epstein Model: Finite Time Stability and Finite Time Synchronization, *Computation*, **12** (2024), 197. http://doi.org/10.3390/computation12100197

23. C. V. Kumar, D. G. Prakasha, N. B. Turki, Exploring the dynamics of fractional-order nonlinear dispersive wave system through homotopy technique, *Open Phys.*, **23** (2025), 20250128. http://doi.org/10.1515/phys-2025-0128

24. C. D. Kumar, D. G. Prakasha, M. R. Amruthalakshmi, A comprehensive study on dynamical analysis and numerical simulation of foam drainage equation using time-fractional derivative, *Franklin Open*, **14** (2025), 100456. http://doi.org/10.1016/j.fraope.2025.100456

25. I. H. Jebril, I. M. Batiha, S. Momani, A. Biswas, Control Strategies for Mittag-Leffler Synchronization in Variable-Order Fractional FitzHugh-Nagumo Reaction-Diffusion Networks, *Contem. Math.*, **61** (2025), 6414–6443. http://doi.org/10.37256/cm.6520257613

26. A. Abbad, S. Bendoukha, S. Abdelmalek, On the local and global asymptotic stability of the Degn–Harrison reaction-diffusion model, *Math. Methods Appl. Sci.*, **42** (2019), 567–577. http://doi.org/10.1002/mma.5362

27. B. Lisena, Some global results for the Degn–Harrison system with diffusion, *Mediterr. J. Math.*, **14** (2017), 91. http://doi.org/10.1007/s00009-017-0894-x

28. J. Zhou, Pattern formation in a general Degn-Harrison reaction model, *Bull. Korean Math. Soc.*, **54** (2017), 655–666. http://doi.org/10.4134/BKMS.b160249

29. R. Mezhoud, K. Saoudi, A. Zaraï, S. Abdelmalek, Conditions for the local and global asymptotic stability of the time–fractional Degn–Harrison system, *Int. J. Nonlinear Sci. Numer. Simul.*, **21** (2020), 749–759. http://doi.org/10.1515/ijnsns-2019-0159

30. S. Li, J. Wu, Y. Dong, Turing patterns in a reaction–diffusion model with the Degn–Harrison reaction scheme, *J. Differ. Equ.*, **259** (2015), 1990–2029. http://doi.org/10.1016/j.jde.2015.03.017

31. P. A. Naik, S. Naveen, V. Parthiban, S. Qureshi, M. Alquran, M. Senol, Advancing Lotka-Volterra system simulation with variable fractional order Caputo derivative for enhanced dynamic analysis, *J. Appl. Anal. Comput.*, **15** (2025), 1002–1019. http://doi.org/10.11948/20240243

32. R. Almeida, Caputo–Hadamard fractional derivatives of variable order, *Numer. Funct. Anal. Optim.*, **38** (2017), 1–19. http://doi.org/10.1080/01630563.2016.1217880

33. S. Sarwar, On the existence and stability of variable order Caputo type fractional differential equations, *Fractal Fract.*, **6** (2022), 51. http://doi.org/10.3390/fractalfract6020051

34. D. Tavares, R. Almeida, D. F. M. Torres, Caputo derivatives of fractional variable order: numerical approximations, *Commun. Nonlinear Sci. Numer. Simul.*, **35** (2016), 69–87. http://doi.org/10.1016/j.cnsns.2015.10.027

35. C. Goodrich, A. C. Peterson, *Discrete Fractional Calculus*, Cham: Springer, 2015. http://doi.org/10.1007/978-3-319-25562-0

36. N. M. Al-Saidi, H. Natiq, R. W. Ibrahim, D. Baleanu, The dynamic and discrete systems of variable fractional order in the sense of the Lozi structure map, *AIMS Mathematics*, **8** (2023), 733–751. http://doi.org/10.3934/math.2023035

37. B. P. Moghaddam, A. Babaei, A. Dabiri, A. Galhano, Fractional stochastic partial differential equations: Numerical advances and practical applications—A state of the art review, *Symmetry*, **16** (2024), 563. http://doi.org/10.3390/sym16050563

38. P. Verma, W. Sumelka, Existence, stability, and numerical methods for multi-fractional integro-differential equations with singular kernel, *Mathematics*, **13** (2025), 2656. http://doi.org/10.3390/math13162656

39. S. Patnaik, F. Semperlotti, Modeling contacts and hysteretic behavior in discrete systems via variable-order fractional operators, *J. Comput. Nonlinear Dyn.*, **15** (2020), 091008. http://doi.org/10.1115/1.4046831

40. A. F. Fareed, E. A. Mohamed, M. Aly, M. S. Semary, A novel numerical method for stochastic conformable fractional differential systems, *AIMS Mathematics*, **10** (2025), 7509–7525. http://doi.org/10.3934/math.2025345

41. A. Salim, J. E. Lazreg, M. Benchohra, On tempered (κ, ϕ)-Hilfer fractional boundary value problems, *Pan-Am. J. Math.*, **3** (2024), 1. http://doi.org/10.28919/cpr-pajm/3-1

42. O. Tunç, New results on the Ulam–Hyers–Mittag–Leffler stability of Caputo fractional-order delay differential equations, *Mathematics*, **12** (2024), 1342. http://doi.org/10.3390/math12091342

43. C. Xu, X. Yang, J. Lu, J. Feng, F. E. Alsaadi, T. Hayat, Finite-time synchronization of networks via quantized intermittent pinning control, *IEEE Trans. Cybern.*, **48** (2017), 3021–3027. http://doi.org/10.1109/TCYB.2017.2749248

44. R. Du, J. Tang, Efficient numerical methods for time-fractional diffusion equations with Caputo-type Erdélyi–Kober operators, *Fractal Fract.*, **9** (2025), 486. http://doi.org/10.3390/fractalfract9080486

Appendix

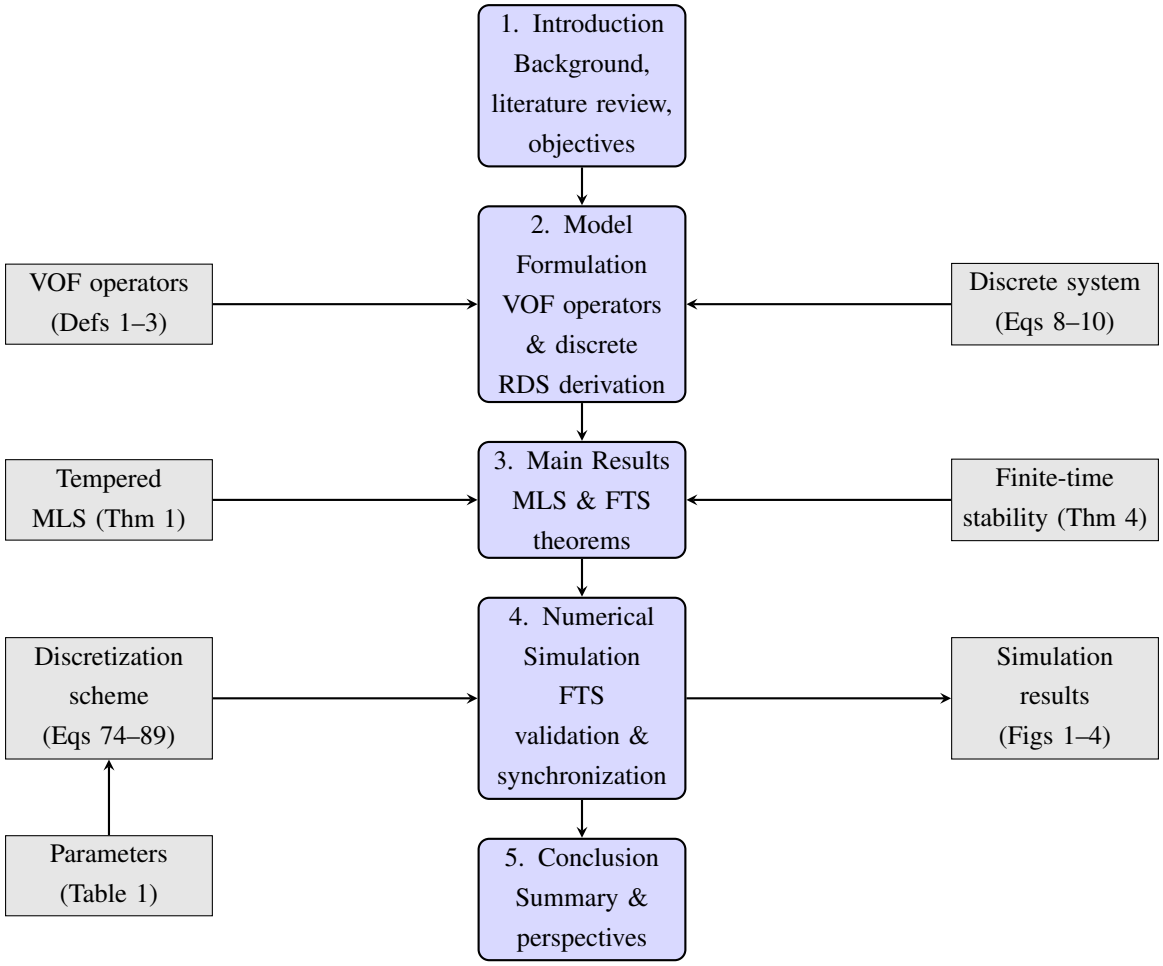

Figure 6. Flowchart of the study structure. Sections 1–5 (rounded rectangles) represent the main progression. Plain boxes show supporting definitions, theorems, schemes, and simulation results.